

Compressing LLMs with MoP: Mixture of Pruners

Bruno Lopes Yamamoto¹ Lucas Lauton de Alcantara¹ Victor Zacarias¹ Leandro Giusti Mugnaini¹
Keith Ando Ogawa¹ Lucas Pellicer² Rosimeire Pereira Costa² Edson Bollis² Anna Helena Reali Costa¹
Artur Jordao¹

Abstract

The high computational demands of Large Language Models (LLMs) motivate methods that reduce parameter count and accelerate inference. In response, model pruning emerges as an effective strategy, yet current methods typically focus on a single dimension—depth or width. We introduce MoP (Mixture of Pruners), an iterative framework that unifies these dimensions. At each iteration, MoP generates two branches—pruning in depth versus pruning in width—and selects a candidate to advance the path. On LLaMA-2 and LLaMA-3, MoP advances the frontier of structured pruning, exceeding the accuracy of competing methods across a broad set of compression regimes. It also consistently outperforms depth-only and width-only pruning. Furthermore, MoP translates structural pruning into real speedup, reducing end-to-end latency by 39% at 40% compression. Finally, extending MoP to the vision-language model LLaVA-1.5, we notably improve computational efficiency and demonstrate that text-only recovery fine-tuning can restore performance even on visual tasks.

1. Introduction

In the rapidly transforming world of computation, large foundational models stand as the primary drivers of cognitive progress, pushing the frontier of machine intelligence to a previously unseen degree (Maslej et al., 2025). Such outstanding performance often entails unintended downsides, especially as models scale in size and cost (Maslej et al., 2025). In this context, model compression serves as an effective means to reduce model size and, in turn, computa-

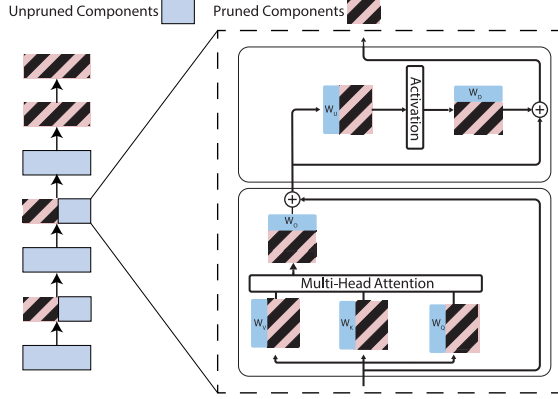


Figure 1. Illustration of MoP combining depth pruning (removing transformer layers) and width pruning (removing attention heads and MLP neurons).

tional demands (Ma et al., 2023; Sreenivas et al., 2024). A practical route to this goal is pruning, particularly structured pruning.

Structured pruning removes coherent structures rather than individual weights (Ma et al., 2023). Unlike unstructured sparsity, these methods do not require specialized hardware or software to realize the speedup and cost reduction (Ashkboos et al., 2024). Within structured pruning, two main approaches emerge. The first removes stacked components (e.g., entire transformer layers) to reduce model depth, resulting in a shallower architecture (depth pruning). The second removes components within layers (e.g., attention heads, MLP neurons) to reduce internal dimensions, resulting in a narrower architecture (width pruning). While width pruning enables finer-grained selection of redundant structures, tending to better preserve performance on downstream tasks (Sreenivas et al., 2024), depth pruning, by reducing sequential computation, often yields superior inference acceleration (Sreenivas et al., 2024).

Building on these complementary strengths, we introduce our Mixture of Pruners (MoP) method, a novel approach to the depth–width dichotomy that synthesizes both benefits through an iterative pruning process. Figure 2 summarizes

¹Universidade de São Paulo, Brazil ²Instituto de Ciência e Tecnologia Itaú (ICTi), Brazil. Correspondence to: <brunolyamamoto@usp.br>.

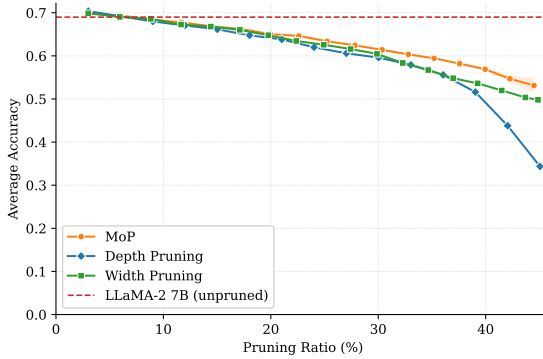


Figure 2. Average accuracy on five standard commonsense benchmarks, comparing depth pruning, width pruning, and MoP (combining both) on LLaMA-2 7B. MoP achieves a Pareto improvement over single-dimension approaches.

the advantages of our strategy and confirms that MoP consistently outperforms both pure depth and pure width pruning across all compression ratios on LLaMA-2 7B, achieving a Pareto improvement over single-dimension approaches.

MoP builds upon existing forms of pruning through an iterative process. At each step, our method evaluates both depth and width candidates, using a criterion to guide the selection. This process repeats until reaching the target compression, followed by recovery fine-tuning. The modular design accommodates different pruning criteria. We further demonstrate that MoP extends to multimodal architectures such as LLaVA (Liu et al., 2024), and we observe that text-only recovery fine-tuning can substantially restore multimodal performance after pruning (see Section 4.4).

Among our contributions, we highlight the following: (1) We propose MoP, an efficient method that effectively combines both depth and width pruning, capturing the advantages of both paradigms: the latency reduction of depth pruning and the fine-grained selectivity of width pruning. (2) MoP follows a modular design, meaning it accommodates other combinations of width and depth pruning criteria. This allows MoP to incorporate future state-of-the-art pruning criteria, possibly further enhancing its performance. (3) MoP provides a more diverse pruning scheme, achieving higher compression ratios by distributing removal across both depth and width rather than exhausting a single dimension. (4) Unlike most pruning literature, we test our method in both language and multimodal architectures. (5) To the best of our knowledge, we are the first to observe that text-only recovery fine-tuning can, surprisingly, restore performance on visual benchmarks in pruned vision-language models.

Code and models are available at: <https://github.com/c2d-usp/Efficient-LLMs-with-MoP>.

2. Related Work

Depth pruning. Within a layer-wise pruning approach, LLM-Streamline (Chen et al., 2025a) measures the importance of layers by assessing the cosine similarity between the input and output hidden states of each of them. The authors argue that a high cosine similarity indicates a nonessential transformation, suggesting that the layer is a strong candidate for pruning. In a different direction, LaCo (Yang et al., 2024) merges layers to achieve model compression. Specifically, the process iteratively merges a set of contiguous layers, assesses whether the merged layer is similar enough to the original set, and selects the next set of layers to merge. To better understand how LLMs store knowledge in their weights, Gromov et al. (Gromov et al., 2025) leverage cosine similarity to analyze layer pruning. Interestingly, they found that, for most architectures, promising pruning sets of layers appear in the deeper part of the neural network. Based on this evidence, the authors show that removing the deepest layers leads to a model with predictive performance on question-answering tasks comparable to carefully selecting with a similarity measure. Building on these findings, we follow a similar strategy for the layer pruning part of our method MoP.

Width pruning. Aiming at attention heads and MLP neurons, AMP (Mugnaini et al., 2025) measures the importance of these components by assessing the magnitude of their activation. The authors associate a lower magnitude of activation with a less important contribution and uniformly prune across all layers. On the other hand, PruneNet (Sengupta et al., 2025) focuses on pruning MLPs by looking at the singular value distribution of their weight matrices. Rather than using data to assess important structures, the authors propose a policy-based technique that learns the rows to prune. ModHiFi (Kashyap et al., 2025) introduces Sub-set Fidelity, a local reconstruction metric with an optimal compensation term to score component importance without gradients. ModHiFi then keeps high-fidelity channels based on scores and prunes the rest using synthetic calibration data.

In contrast to previous work, MoP benefits from characteristics of both types of structured pruning strategies. More concretely, our method leverages the superior inference acceleration of layer-wise pruning and the finer granularity of component-wise pruning. We also extend our method to visual-language architectures.

3. Proposed Mixture of Pruners (MoP) method

3.1. Transformer Architecture

Depth Aspects. Most modern language transformers employ a decoder-only architecture (Grattafiori et al., 2024;

Touvron et al., 2023b;a; Li et al., 2023), essentially containing a single deep stack of layers that consecutively transform the input into a meaningful final representation. Therefore, model depth depends on the number of stacked layers. Each layer shares the same general structure: an attention module and a multi-layer perceptron (MLP), with normalization and skip connections. Importantly, all layers share the same dimensions. This leads to two key consequences for depth pruning. First, depth-wise pruning removes layers without changing the model architecture or adding extra parameters, since the inputs and outputs of every layer are dimensionally compatible. Second, the full layer is the smallest removable depth unit that still preserves model structure, since removing internal components (e.g., the MLP or attention module) would make the architecture non-uniform across layers.

Width Aspects. In a transformer layer, most parameters belong to the attention module and the MLP. Naturally, these modules are the usual target for pruning methods within a layer (Mugnaini et al., 2025; Sengupta et al., 2025). In the attention and MLP modules, all learnable parameters reside in the linear projection matrices. Width pruning, therefore, consists of reducing the internal dimensions of these matrices by removing whole units (e.g., attention heads or MLP neurons), thereby reducing their size. In most cases, width pruning narrows only the internal widths, thus keeping input and output compatibility between layers. Since width pruning works on internal dimensions, which are typically in the thousands, it allows much finer granularity, for example, acting at the level of individual neurons in the MLP. Overall, depth and width pruning methods operate on different axes: the former reduces the transformer by decreasing the number of stacked layers, whereas the latter decreases the dimensions of the wide projection matrices inside each layer to obtain a narrower structure. Figure 1 illustrates this distinction.

3.2. Proposed method

For clarity, we first describe the general MoP framework under generic width and depth pruning criteria, and then instantiate it with the specific choices adopted in this work.

Width and Depth pruning. For the depth-wise pruning, we choose to remove at each step one complete transformer layer. This choice provides the minimal pruning unit along the depth dimension, since removing submodules inside a transformer layer (e.g., entire linear projections in the attention or MLP) would either make internal dimensions incompatible or remove essential transformer structures.

In the case of width pruning, MoP works with any width pruning method that provides enough granularity in the pruning ratio (i.e., small steps). This contrasts with the coarse jumps in model size that layer removal produces. As we shall see, this condition is necessary so that we can

Algorithm 1 Pruning with MoP

Input: Unpruned model \mathcal{F} , Target compression ratio ρ , Training samples \mathcal{D} with labels \mathbf{Y} , Fixed calibration set \mathcal{D}_{cal} , Path criterion \mathcal{P} , Width pruning criterion \mathcal{W} , Layer pruning criterion \mathcal{L}

Output: \mathcal{F}' (Pruned version of \mathcal{F})

- 1: $\mathcal{F}^{(0)} \leftarrow \mathcal{F}$ ▷ Initialise current model
- 2: $t \leftarrow 1$
- 3: $P_{\min} \leftarrow (1 - \rho) \cdot \text{TOTALPARAMS}(\mathcal{F})$ ▷ Target parameter count
- 4: **while** $\text{TOTALPARAMS}(\mathcal{F}^{(t-1)}) > P_{\min}$ **do**
- 5: $\mathcal{D}_{\text{tune}}^{(t)} \leftarrow \text{SAMPLETUNESUBSET}(\mathcal{D})$ ▷ Iteration-dependent fine-tuning subset
- 6: $\ell^* \leftarrow \mathcal{L}(\mathcal{F}^{(t-1)})$ ▷ Select one layer to remove
- 7: $p_{\ell} \leftarrow \text{LAYERPARAMS}(\mathcal{F}^{(t-1)}, \ell^*)$ ▷ Parameter count of the selected layer
- 8: $c_t \leftarrow p_{\ell} / \text{TOTALPARAMS}(\mathcal{F}^{(t-1)})$ ▷ Compression ratio based on that layer
- 9: ▷ Width-level candidate
- 10: $\Omega \leftarrow \mathcal{W}(\mathcal{F}^{(t-1)}, \mathcal{D}_{\text{cal}})$ ▷ Score width units by \mathcal{W} on calibration data
- 11: $\mathcal{F}_{\text{width}} \leftarrow \text{WIDTHPRUNE}(\mathcal{F}^{(t-1)}, \Omega, c_t)$
- 12: $\tilde{\mathcal{F}}_{\text{width}} \leftarrow \text{FINETUNE}(\mathcal{F}_{\text{width}}, \mathcal{D}_{\text{tune}}^{(t)})$
- 13: $s_{\text{width}} \leftarrow \mathcal{P}(\tilde{\mathcal{F}}_{\text{width}}, \mathcal{F}, \mathcal{D}_{\text{cal}})$ ▷ Compare against original model
- 14: ▷ Layer-level candidate
- 15: $\mathcal{F}_{\text{layer}} \leftarrow \text{LAYERPRUNE}(\mathcal{F}^{(t-1)}, \ell^*)$
- 16: $\tilde{\mathcal{F}}_{\text{layer}} \leftarrow \text{FINETUNE}(\mathcal{F}_{\text{layer}}, \mathcal{D}_{\text{tune}}^{(t)})$
- 17: $s_{\text{layer}} \leftarrow \mathcal{P}(\tilde{\mathcal{F}}_{\text{layer}}, \mathcal{F}, \mathcal{D}_{\text{cal}})$ ▷ Compare against original model
- 18: ▷ Path decision
- 19: **if** $s_{\text{width}} \leq s_{\text{layer}}$ **then**
- 20: $\mathcal{F}^{(t)} \leftarrow \mathcal{F}_{\text{width}}$
- 21: **else**
- 22: $\mathcal{F}^{(t)} \leftarrow \mathcal{F}_{\text{layer}}$
- 23: **end if**
- 24: $t \leftarrow t + 1$
- 25: **end while**
- 26: $\mathcal{F}' \leftarrow \text{FINETUNE}(\mathcal{F}^{(t-1)}, \mathcal{D}, \mathbf{Y})$

match the number of parameters pruned when removing a layer or pruning in width.

MoP algorithm. We build our method upon the idea of exploring the advantages of pruning structures at different granularities (i.e., layers and their width components), challenging the current dichotomy of depth and width pruning. Instead of removing only one type of component, we propose to iteratively evaluate both based on existing pruning criteria. This modular approach allows us to integrate new pruning strategies for width or depth into our method. Formally, given a model \mathcal{F} and a pair of pruning methods, one for width and one for depth, to achieve a desired compression ratio, we iteratively prune the model. At each iteration, a path criterion \mathcal{P} decides which type of pruning to apply, resulting in a final model that combines both strategies.

A question that arises is how much to prune at each itera-

tion. We want the smallest step possible to maintain fine control over the pruning trajectory. The minimum for layer pruning is one layer, so we use this as the basis and prune the equivalent number of parameters in width, this ensures a fair comparison between both candidates. Since width pruning is more fine-grained, it can approximate the number of parameters of one layer. At each iteration, we first identify the layer ℓ^* selected by criterion \mathcal{L} , then compute c_t as the fraction of parameters that the selected layer represents (line 8 in Algorithm 1). Importantly, we recompute c_t at each iteration since width pruning changes the number of parameters per layer. This ensures that we compare both candidates on a consistent basis, removing the same number of parameters at each iteration.

Algorithm 1 details our method. At each iteration t , we create two candidate models: one by applying width pruning with ratio c_t and one by removing a single layer. The width criterion \mathcal{W} produces the width candidate $\mathcal{F}_{\text{width}}$, and the layer criterion \mathcal{L} selects which layer to remove, producing $\mathcal{F}_{\text{layer}}$. We then apply a short recovery fine-tuning step to both candidates on a training subset $\mathcal{D}_{\text{tune}}^{(t)}$ before evaluation. The path criterion \mathcal{P} scores the corresponding fine-tuned candidates $\tilde{\mathcal{F}}_{\text{width}}$ and $\tilde{\mathcal{F}}_{\text{layer}}$ against the original (unpruned) model and decides whether width or depth pruning defines the next model $\mathcal{F}^{(t)}$. We set $\mathcal{F}^{(t)}$ to the corresponding pruned model *before* this short update, $\mathcal{F}_{\text{width}}$ or $\mathcal{F}_{\text{layer}}$, discarding the intermediate fine-tuning, serving only to assess the relative quality of the candidates. The process repeats until we reach the desired compression, and we then apply full fine-tuning to the final model on the complete training set \mathcal{D} .

The Layer criterion. Recent literature on layer pruning explores data-driven methods for ascertaining redundancy in transformer layers (Gromov et al., 2025; Chen et al., 2025a). These methods, based on criteria such as cosine similarity, converge to a common finding: the deeper layers in the model tend to be more redundant, with the exception of the very last, which is essential due to its proximity to the output projection. According to Gromov et al. (Gromov et al., 2025), their data-driven approach actually leads to a simple algorithm: prune from the penultimate layer to the first. Kim et al. (Kim et al., 2024) use a slightly higher margin and preserve the last two layers instead of just one. Following these insights from the literature, we adopt as our layer criterion \mathcal{L} the following procedure. At each iteration, the criterion \mathcal{L} selects the third-to-last layer for pruning. This guarantees that we always keep the last two layers and that we remove layers from the end to the beginning.

The Width Criterion. Adhering to the requirements of fine-grained compression control and strong empirical performance, we adopt AMP (Mugnaini et al., 2025) as the width pruning criterion \mathcal{W} . AMP removes attention heads

and MLP neurons uniformly across layers. This neuron-level pruning enables MoP to precisely match the parameter count of a single layer at each iteration, ensuring fair comparisons between width and depth candidates. Additionally, AMP outperforms several width pruning methods on benchmarks for the LLaMA family (Mugnaini et al., 2025).

The Path Criterion. At each iteration, MoP must decide whether to apply width or depth pruning. A path criterion \mathcal{P} governs this decision and evaluates both candidate models ($\tilde{\mathcal{F}}_{\text{width}}$ and $\tilde{\mathcal{F}}_{\text{layer}}$) and selects the one that best preserves the original model’s capabilities. We define \mathcal{P} to output a single scalar score that measures how much a candidate deviates from the original (unpruned) model, where smaller scores indicate closer behavior and are therefore preferred. To ensure a fair comparison between candidates, MoP prunes both with the same compression ratio c_t , removing an equivalent number of parameters regardless of the pruning type.

MoP is modular in its choice of path criterion \mathcal{P} . In this work, we instantiate \mathcal{P} with commonly used metrics (Agarwal et al., 2024; Muralidharan et al., 2024; Gromov et al., 2025; Kim et al., 2024; Mugnaini et al., 2025; Chen et al., 2025a), including cosine similarity, KL divergence, and perplexity, and we also test randomized path selection.

3.3. Path Selection Strategies

We explore three distinct metrics for \mathcal{P} : cosine similarity, Kullback–Leibler (KL) divergence, and perplexity (PPL). These rely on a simple forward pass with the calibration data subset. In all cases, lower values indicate closer agreement with the reference model. We also test random selection as a baseline.

Cosine similarity. We compute the angle (Gromov et al., 2025) between the flattened output logits of the reference and pruned models, \mathbf{v}_{ref} and $\mathbf{v}_{\text{pruned}}$:

$$\theta = \arccos \left(\frac{\mathbf{v}_{\text{ref}} \cdot \mathbf{v}_{\text{pruned}}}{\|\mathbf{v}_{\text{ref}}\|_2 \|\mathbf{v}_{\text{pruned}}\|_2} \right). \quad (1)$$

Kullback–Leibler divergence. We adopt Kullback–Leibler (Agarwal et al., 2024; Muralidharan et al., 2024) divergence to measure the distributional shift between the output token probabilities of the reference (unpruned) and pruned models. Let p and q denote the corresponding softmax distributions over the vocabulary \mathcal{V} . We compute the average divergence across N sequence positions:

$$D_{KL}(p\|q) = \frac{1}{N} \sum_{i=1}^N \sum_{x \in \mathcal{V}} p_i(x) \log \left(\frac{p_i(x)}{q_i(x)} \right). \quad (2)$$

Perplexity. We compute perplexity of the candidate model on calibration data (Gromov et al., 2025; Kim et al., 2024;

Table 1. Performance comparison of path selection criteria for MoP on LLaMA 7B at a 30% compression ratio. We highlight the highest accuracy across criteria in bold.

Method	WinoGrande	HellaSwag	ARC-e	ARC-c	PIQA	Avg
KL	65.27	63.42	58.50	37.88	71.00	59.21
Cosine	62.19	67.58	62.71	37.46	73.45	60.68
PPL	63.69	66.35	62.54	38.14	73.50	60.84
Random	63.14±0.91	66.47±0.38	63.01±0.52	37.71±0.60	73.81±0.60	60.83±0.43

Mugnaini et al., 2025), measuring how well the compressed model predicts a sequence of tokens $X = (x_1, \dots, x_T)$:

$$\text{PPL}(X) = \exp \left(-\frac{1}{T} \sum_{t=1}^T \log P(x_t | x_1, \dots, x_{t-1}) \right). \quad (3)$$

Randomized Path Selection. As an alternative to metric-based selection, we also evaluate a randomized criterion that chooses between width and depth pruning with equal probability at each iteration.

4. Experiments

4.1. Experimental Settings

Notable models. We evaluate MoP on four well-established architectures: the language-only models LLaMA 7B (Touvron et al., 2023b), LLaMA-2 7B (Touvron et al., 2023a), LLaMA-3 8B (Grattafiori et al., 2024), and the multimodal vision-language model LLaVA-1.5 7B (Liu et al., 2024). LLaMA 7B serves exclusively for calibration experiments.

Evaluation setup. Building upon previous efforts (Ma et al., 2023; Kim et al., 2024; Gao et al., 2024; Ashkboos et al., 2024; van der Ouderaa et al., 2024; Mugnaini et al., 2025), we evaluate the LLMs on five commonsense benchmarks: ARC-e / ARC-c (Clark et al., 2018), HellaSwag (Zellers et al., 2019), PIQA (Bisk et al., 2020), and WinoGrande (Sakaguchi et al., 2020). We employ the EleutherAI LM Harness framework (Gao et al., 2021) to conduct these evaluations. Consistent with established literature (van der Ouderaa et al., 2024; Mugnaini et al., 2025), we report standard accuracy for WinoGrande and normalized accuracy for the remaining tasks. For the multimodal architecture LLaVA-1.5 (Liu et al., 2024), we adopt the LMMs-Eval framework (Zhang et al., 2025) to measure performance on four prominent (Guo et al., 2025b; Luo et al., 2025; Zhao et al., 2024; Chow et al., 2024) multimodal datasets: ScienceQA (Lu et al., 2022), VizWiz (Gurari et al., 2018), LLaVA-Bench (In-the-Wild) (Liu et al., 2023), and MM-Vet (Yu et al., 2024). We report the official metric for each benchmark.

Post-training setup. Adhering to standard practices in the literature (Ashkboos et al., 2024; Sengupta et al., 2025; Fu et al., 2024; Mugnaini et al., 2025; Guo et al., 2025a; Kim

et al., 2024; Gao et al., 2024), we perform recovery fine-tuning (RFT) on the Alpaca dataset via Low-Rank Adaptation (LoRA) (Hu et al., 2022). For the language models, we fix the rank (r) at 32 and alpha (α) at 10, consistent with previous works (Gao et al., 2024; Ashkboos et al., 2024). Furthermore, we employ the AdamW optimizer with a learning rate of 3e-4, a batch size of 16 and train over two epochs, following standard practices (Ma et al., 2023; Mugnaini et al., 2025). For multimodal models, we observe that standard fine-tuning on Alpaca suffices to recover performance (details in Section 4.4). We therefore retain the LLM configurations, modifying only the rank to 8 and alpha to 16. This adjustment adheres to common literature practices (Ma et al., 2023; Kim et al., 2024; Mugnaini et al., 2025). We train both model families using an RTX 4090 GPU. On this hardware, one MoP run to a target compression ratio (including recovery fine-tuning) completes in just 2 hours.

Criteria assessment and intermediate fine-tuning. We perform all metric evaluations on the WikiText-2 (Merity et al., 2017) test set, consistent with its standard use as calibration data (Ashkboos et al., 2024; Sengupta et al., 2025; Kashyap et al., 2025; Fu et al., 2024; Yang et al., 2025; Kim et al., 2024; Guo et al., 2025a; Chen et al., 2025b). For cosine similarity and Kullback-Leibler divergence, we select 128 random non-empty texts (Ashkboos et al., 2024; Chen et al., 2025b; Kashyap et al., 2025). Conversely, perplexity evaluation involves the full test split, processed in fixed segments of 2048 tokens to capture long-range dependencies (Ashkboos et al., 2024). As pruning progressively degrades model capabilities, comparing candidates in their raw state yields unreliable predictions of their final post-recovery performance. To mitigate this discrepancy, we apply a dynamic alignment rule: at pruning iteration i , we execute $10 \times i$ fine-tuning steps on Alpaca, adhering to the configuration detailed in Section 4.1. This protocol balances the necessity of restoring minimal model alignment for accurate path selection with the constraint of computational efficiency.

4.1.1. COMPARISON OF PATH SELECTION STRATEGIES.

To evaluate the efficacy of the proposed path selection criteria, we compare cosine, KL, PPL, and a random selector at 30% compression on LLaMA 7B. We report random path as mean and standard deviation over three runs (Table 1). Across these runs, randomized selection performs on par with PPL and cosine and exceeds KL. Given these results, we adopt random selection as the criterion for the path. This also reduces the computational overhead of the metric calculations. We treat it as a conservative lower bound on MoP’s capability, as MoP is modular and supports stronger future path criteria as drop-in replacements. For all subsequent experiments, we report results over three independent random pruning paths. This finding suggests that the carefully

Table 2. Performance of MoP relative to other state-of-the-art pruning methods. We highlight the best results in bold for each compression ratio and model.

Pruning Ratio	Method	WinoGrande	HellaSwag	ARC-e	ARC-c	PIQA	Avg
0%	LLaMA-2 7B	69.14	75.99	74.58	46.15	79.11	68.99
20%	SliceGPT (Ashkboos et al., 2024) (ICLR, 2024)	65.11	59.04	59.76	37.54	69.42	58.18
	AmoebaLLM (Fu et al., 2024) (NeurIPS, 2024)	66.90	70.80	70.30	40.20	76.30	64.90
	PruneNet (Sengupta et al., 2025) (ICLR, 2025)	66.22	68.37	63.93	38.40	74.76	62.34
	SlimLLM (Guo et al., 2025a) (ICML, 2025)	64.88	70.95	67.17	38.99	78.02	64.00
	ModHiFi-P (Kashyap et al., 2025) (NeurIPS, 2025)	64.64	62.70	64.73	38.22	72.79	60.62
	CoMe (Wang et al., 2025) (NeurIPS, 2025)	67.25	68.68	64.10	39.59	72.42	62.41
	LINEARPATCH (Chen et al., 2025b) (NeurIPS, 2025)	67.40	69.33	64.35	38.23	73.23	62.51
	AMP (Mugnaini et al., 2025) (IJCNN, 2025)	61.56	69.22	68.18	42.06	76.39	63.48
	MoP (Ours)	65.19 \pm 1.12	71.16\pm0.51	70.54\pm0.60	42.86\pm0.32	76.35 \pm 0.06	65.22\pm0.21
30%	SliceGPT (Ashkboos et al., 2024) (ICLR, 2024)	61.33	49.62	51.77	31.23	63.55	51.50
	Shortened LLaMA (Kim et al., 2024) (ICLR, 2024)	61.09	54.97	45.96	34.81	60.99	51.56
	DISP-LLM (Gao et al., 2024) (NeurIPS, 2024)	63.93	62.87	60.10	37.03	73.72	59.53
	PruneNet (Sengupta et al., 2025) (ICLR, 2025)	62.90	63.21	53.37	33.70	72.20	57.08
	Yang et al. (Yang et al., 2025) (ICML, 2025)	60.77	59.18	58.16	34.22	70.95	56.65
	ModHiFi-P (Kashyap et al., 2025) (NeurIPS, 2025)	59.35	50.61	53.15	32.50	66.59	52.44
	CoMe (Wang et al., 2025) (NeurIPS, 2025)	63.38	65.83	63.51	35.58	74.05	60.47
	LINEARPATCH (Chen et al., 2025b) (NeurIPS, 2025)	66.69	64.52	60.65	34.81	70.29	59.39
	AMP (Mugnaini et al., 2025) (IJCNN, 2025)	61.25	65.47	64.31	39.85	74.21	61.02
	MoP (Ours)	62.38 \pm 1.87	66.88\pm0.21	65.38\pm0.44	39.36 \pm 0.13	73.72 \pm 0.38	61.54\pm0.27
40%	Yang et al. (Yang et al., 2025) (ICML, 2025)	56.67	49.00	49.83	30.38	66.10	50.39
	AMP (Mugnaini et al., 2025) (IJCNN, 2025)	52.96	55.44	55.43	32.42	69.04	53.06
	MoP (Ours)	59.35\pm1.32	57.94\pm0.43	57.05\pm1.20	34.16\pm0.80	68.36 \pm 0.97	55.37\pm0.45
0%	LLaMA-3 8B	72.77	79.19	77.78	52.90	80.85	72.70
20%	LINEARPATCH (Chen et al., 2025b) (NeurIPS, 2025)	70.17	66.74	60.82	43.17	72.85	62.75
	CoMe (Wang et al., 2025) (NeurIPS, 2025)	70.96	65.52	64.23	40.44	73.50	62.93
	AMP (Mugnaini et al., 2025) (IJCNN, 2025)	59.91	66.53	67.68	44.20	75.30	62.72
	MoP (Ours)	66.80 \pm 1.34	71.94\pm0.13	67.94\pm1.45	44.62\pm0.77	75.88\pm1.80	65.44\pm1.04
30%	CoMe (Wang et al., 2025) (NeurIPS, 2025)	60.62	50.42	50.67	33.70	67.08	52.50
	Yang et al. (Yang et al., 2025) (ICML, 2025)	60.30	54.40	54.76	33.19	69.10	54.34
	AMP (Mugnaini et al., 2025) (IJCNN, 2025)	60.77	61.93	59.76	35.84	71.76	58.01
	MoP (Ours)	63.75\pm0.67	65.44\pm0.72	61.98\pm1.63	38.77\pm1.03	72.22\pm0.30	60.43\pm0.59
40%	Yang et al. (Yang et al., 2025) (ICML, 2025)	56.27	44.74	46.51	27.30	64.20	47.80
	AMP (Mugnaini et al., 2025) (IJCNN, 2025)	56.91	52.96	52.74	33.28	67.36	52.65
	MoP (Ours)	61.38\pm0.81	56.27\pm1.78	56.52\pm2.99	34.67\pm0.83	67.85\pm1.05	55.34\pm1.42

designed matching of pruned parameters in depth and width at each step of MoP is enough to make either path similarly strong, while also substantially improving model performance compared with following only depth or only width, as Figure 2 demonstrates.

4.2. Zero-Shot Performance

Table 2 compares MoP against other pruning methods ¹. According to this table, MoP ranks first at 20%, 30%, and 40% compression on both LLaMA-2 7B and LLaMA-3 8B. This tier-wide sweep shifts the interpretation from isolated wins to a robustness guarantee: even the worst MoP seed exceeds the strongest reported baseline mean at the same tier, so MoP does not rely on favorable path selection to achieve state-of-the-art accuracy.

¹For Shortened LLaMA, we use results from AMP (Mugnaini et al., 2025), who ran this method since the original authors do not evaluate this model. For AMP at compression tiers not covered in the original paper, we run the method ourselves. Apart from that, not all methods appear in every comparison, as some original publications do not report results for all models or compression tiers.

On LLaMA-2 7B, the worst-seed mean accuracy remains 64.97% at 20%, 61.24% at 30%, and 54.97% at 40%. These values exceed the best baseline means at each tier, including AmoebaLLM at 20% (64.90%) and AMP at 30% and 40% (61.02% and 53.06%). The margins become pronounced as compression increases: the worst-seed advantage grows from 0.07 percentage points (pp) at 20% to 1.91 pp at 40%, and the full MoP mean remains higher still. This pattern indicates that MoP preserves accuracy under progressively tighter capacity constraints instead of trading reliability for compression.

LLaMA-3 8B amplifies the same conclusion. The worst-seed mean accuracy reaches 64.33% at 20%, 59.87% at 30%, and 54.35% at 40%, exceeding the strongest baselines by 1.40 pp at 20% (CoMe (Wang et al., 2025) at 62.93%), 1.86 pp at 30% (AMP (Mugnaini et al., 2025) at 58.01%), and 1.70 pp at 40% (AMP (Mugnaini et al., 2025) at 52.65%). This dominance becomes even sharper when benchmarked against the third-place method at each tier: the margin expands from 1.58 pp at 20% (LINEARPATCH (Chen et al., 2025b)) to 5.53 pp at 30% and 6.55 pp at 40% (both Yang et al. (Yang et al., 2025)). Overall, the worst-seed evaluation

removes seed selection as an implicit hyperparameter and points out that MoP delivers top-tier accuracy across tiers even under the least favorable path selection.

Figure 2 further substantiates the central mechanism behind these gains. When we restrict MoP to prune only in depth or only in width across iterations, the mixed strategy consistently outperforms both single-dimension variants. Collectively, these results confirm that effectively exploiting the complementarity between width and depth establishes a new state-of-the-art, delivering resilient performance retention even where other strategies falter.

4.3. Inference Speedup

Practical inference acceleration depends on two critical factors: minimizing the memory bandwidth required to move model weights and shortening the sequential critical path of the forward pass (Sheng et al., 2023; Muralidharan et al., 2024). MoP optimizes both dimensions simultaneously by removing attention heads, MLP neurons, and entire layers, effectively transforming the original architecture into a leaner dense model that retains computational regularity (Ma et al., 2023; Muralidharan et al., 2024). This explicit structural reduction eliminates the computational overhead of the excised components entirely (Ma et al., 2023; Muralidharan et al., 2024). Such efficiency proves decisive not only for meeting strict latency budgets in real-time applications but also for advancing Green AI goals by materially reducing the energy consumption of large-scale model deployment (Sheng et al., 2023; Schwartz et al., 2020).

Following Kim et al. (Kim et al., 2024), we compute latency on a single NVIDIA RTX 4090 GPU. We define the inference task as processing a prompt of 12 input tokens to autoregressively generate 128 output tokens, using a batch size of 1. To ensure stability, we execute 20 independent runs, discarding the first 10 as warm-up and reporting the mean wall-clock time of the remaining 10. Under this protocol, the dense LLaMA-2 7B model establishes a baseline latency of 2.21s. Relative to this baseline, the pruned models at 20%, 30%, and 40% compression rates achieve latencies of (1.82 ± 0.01) s, (1.60 ± 0.03) s, and (1.36 ± 0.03) s, respectively. Such reductions correspond to speedups of $(1.22 \pm 0.01) \times$, $(1.38 \pm 0.02) \times$, and $(1.63 \pm 0.04) \times$, equivalent to end-to-end latency reductions of $(18.0 \pm 0.7)\%$, $(27.5 \pm 1.1)\%$, and $(38.7 \pm 1.5)\%$, respectively. Comparative analysis reveals that at the 20% compression tier, MoP outperforms AMP ($1.19 \times$) and Shortened LLaMA ($1.13 \times$). Furthermore, our method demonstrates superior efficiency against Yang et al. (Yang et al., 2025): the $1.38 \times$ speedup of MoP at 30% compression distinctively surpasses their reported $1.17 \times$ at the same tier and effectively outperforms the $1.30 \times$ speedup they achieve at the far more aggressive 50% compression level.

4.4. MoP on Multimodal Architectures

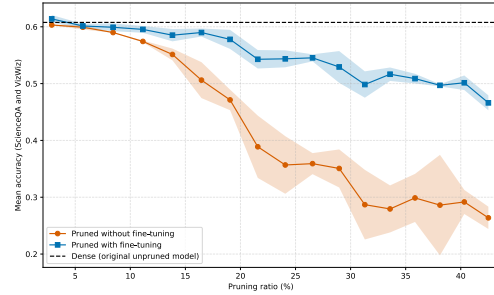


Figure 3. Impact of pruning on LLaVA-1.5 7B with MoP and recovery with text-only fine-tuning. We present the mean accuracy of three runs for ScienceQA and VizWiz across varying compression ratios. Shaded regions denote the standard deviation.

Regarding multimodal architectures, we evaluate the performance of MoP on LLaVA-1.5 7B. Figure 3 illustrates the average accuracy across the ScienceQA and VizWiz datasets for the first 17 iterations of the MoP algorithm. The divergence between the fine-tuned and non-fine-tuned curves emphasizes the necessity of recovery fine-tuning in multimodal pruning and reveals a compelling insight: Alpaca, a dataset designed for text-only models, effectively extends its recovery capabilities to multimodal architectures on visual tasks. To the best of our knowledge, we are the first to document that text-only recovery fine-tuning restores performance in pruned vision-language models. As pruning progresses, the performance gap between the recovered models and their unrefined counterparts becomes pronounced, reaching a peak of 23.71 pp. This disparity extends to stability: while the unrefined models exhibit significant volatility, reaching a standard deviation of 8.85 pp, the fine-tuned variants remain robust, limiting the standard deviation peak to 2.80 pp. Taken together, this experiment underscores the critical role of recovery fine-tuning in the multimodal pruning domain—an area currently under-explored relative to its LLM counterpart—and substantiates the proficiency of Alpaca for RFT despite its text-only origins.

Particularly, Table 3 details the performance of MoP across three distinct compression regimes: 20%, 30%, and 40%. The analysis expands to include MM-Vet and LLaVA-Bench (In-the-Wild), datasets that introduce significant text generation challenges. Despite this increased complexity, MoP demonstrates significant resilience at 20% compression, re-

Table 3. MoP results on LLaVA-1.5 7B across varying compression rates.

Compression	ScienceQA	VizWiz	MM-Vet	LLaVA-Bench	Mean
0%	68.02	53.52	28.44	59.80	52.44
20%	62.96 ± 0.33	45.60 ± 3.30	23.26 ± 0.38	55.00 ± 1.35	46.70 ± 0.96
30%	61.00 ± 1.87	44.86 ± 3.93	21.94 ± 1.08	50.63 ± 1.66	44.61 ± 1.98
40%	57.13 ± 2.57	43.16 ± 4.78	18.88 ± 1.75	44.27 ± 0.91	40.86 ± 1.22

taining 81.79% of its original capability on MM-Vet and 91.97% on LLaVA-Bench (In-the-Wild). At 30% compression, LLaVA-1.5 exhibits a mean performance drop of 7.83 pp relative to the dense baseline. This decline closely parallels the 7.45 pp drop observed in LLaMA-2 7B at the same compression rate, indicating a consistent degradation pattern across distinct modalities despite the difference in benchmarks. Even at the 40% compression tier, the model preserves 77.92% of its mean predictive capabilities. These findings confirm the viability of MoP in diverse compression scenarios and highlight its ability to reduce parameter counts while preserving the core reasoning structures in a multimodal scenario.

5. Conclusions

Current structured pruning strategies often hit a performance ceiling by restricting the search space to a single axis, either thinning the model width or shortening its depth. MoP overcomes this structural rigidity by unifying both approaches into a cohesive, hybrid strategy. Our results demonstrate that this joint pruning yields exceptional resilience: MoP exhibits such stability that its worst-performing path consistently exceeds the average performance of competing methods. This advantage is particularly distinct on LLaMA-3 8B and becomes increasingly pronounced on LLaMA-2 7B as compression intensifies, confirming that the hybrid approach secures robustness exactly where high-compression regimes typically degrade reliability.

Beyond text-only benchmarks, we establish the versatility of MoP in the multimodal domain. By pruning LLaVA-1.5, we effectively preserve performance on visual reasoning tasks, demonstrating a zero-shot cross-modal transferability that purely data-driven, component-specific methods often lack. Furthermore, MoP translates compression into tangible acceleration. The method achieves a $1.38\times$ speedup at 30% compression, outperforming the $1.30\times$ speedup that Yang et al. (Yang et al., 2025) achieve only at a far more aggressive 50% compression level. Collectively, these findings validate the hybrid width-depth paradigm as the superior standard for efficient LLMs and a promising avenue for the multimodal domain.

6. Acknowledgments

The authors would like to thank Instituto de Ciéncia e Tecnologia Itaú (ICTi) and Programa de Bolsas Itaú (PBI). This study was financed, in part, by the São Paulo Research Foundation (FAPESP), Brasil. Process Number #2023/11163-0. This study was financed in part by the Coordenação de Aperfeiçoamento de Pessoal de Nível Superior – Brasil (CAPES) – Finance Code 001. The authors would like to thank grant #402734/2023-8, National Council for Scientific and Tech-

nological Development (CNPq). Anna H. Reali Costa would like to thank grant #312360/2023-1 CNPq.

References

Agarwal, R. et al. On-Policy Distillation of Language Models: Learning from Self-Generated Mistakes. In *International Conference on Learning Representations (ICLR)*, 2024.

Ashkboos, S. et al. SliceGPT: Compress Large Language Models by Deleting Rows and Columns. In *International Conference on Learning Representations (ICLR)*, 2024.

Bisk, Y. et al. PIQA: Reasoning about Physical Commonsense in Natural Language. In *AAAI Conference on Artificial Intelligence (AAAI)*, 2020.

Chen, X. et al. Streamlining Redundant Layers to Compress Large Language Models. In *International Conference on Learning Representations (ICLR)*, 2025a.

Chen, X. et al. A Simple Linear Patch Revives Layer-Pruned Large Language Models. In *Neural Information Processing Systems (NeurIPS)*, 2025b.

Chow, W. et al. Unified Generative and Discriminative Training for Multi-modal Large Language Models. In *Neural Information Processing Systems (NeurIPS)*, 2024.

Clark, P. et al. Think you have Solved Question Answering? Try ARC, the AI2 Reasoning Challenge. *arXiv*, 2018.

Fu, Y. et al. AmoebaLLM: Constructing Any-Shape Large Language Models for Efficient and Instant Deployment. In *Neural Information Processing Systems (NeurIPS)*, 2024.

Gao, L. et al. A framework for few-shot language model evaluation. *Zenodo*, 2021.

Gao, S. et al. DISP-LLM: Dimension-independent structural pruning for large language models. In *Neural Information Processing Systems (NeurIPS)*, 2024.

Grattafiori, A. et al. The llama 3 herd of models. *arXiv*, 2024.

Gromov, A. et al. The Unreasonable Ineffectiveness of the Deeper Layers. In *International Conference on Learning Representations (ICLR)*, 2025.

Guo, J., Chen, X., Tang, Y., and Wang, Y. SlimLLM: Accurate Structured Pruning for Large Language Models. In *International Conference on Machine Learning (ICML)*, 2025a.

Guo, Y. et al. Dynamic Mixture of Experts: An Auto-Tuning Approach for Efficient Transformer Models. In *International Conference on Learning Representations (ICLR)*, 2025b.

Gurari, D. et al. VizWiz Grand Challenge: Answering Visual Questions from Blind People. In *Conference on Computer Vision and Pattern Recognition (CVPR)*, 2018.

Hu, E. J. et al. LoRA: Low-Rank Adaptation of Large Language Models. In *International Conference on Learning Representations (ICLR)*, 2022.

Kashyap, D. et al. ModHiFi: Identifying High Fidelity predictive components for Model Modification. In *Neural Information Processing Systems (NeurIPS)*, 2025.

Kim, B.-K. et al. Shortened LLaMA: A Simple Depth Pruning for Large Language Models. In *International Conference on Learning Representations (ICLR) - Workshop*, 2024.

Li, Y. et al. Textbooks Are All You Need II: phi-1.5 technical report. *arXiv*, 2023.

Liu, H., Li, C., Wu, Q., and Lee, Y. J. Visual Instruction Tuning. In *Neural Information Processing Systems (NeurIPS)*, 2023.

Liu, H., Li, C., Li, Y., and Lee, Y. J. Improved Baselines with Visual Instruction Tuning. In *Conference on Computer Vision and Pattern Recognition (CVPR)*, 2024.

Lu, P. et al. Learn to Explain: Multimodal Reasoning via Thought Chains for Science Question Answering. In Oh, A. H., Agarwal, A., Belgrave, D., and Cho, K. (eds.), *Neural Information Processing Systems (NeurIPS)*, 2022.

Luo, G. et al. Feast Your Eyes: Mixture-of-Resolution Adaptation for Multimodal Large Language Models. In *International Conference on Learning Representations (ICLR)*, 2025.

Ma, X., Fang, G., and Wang, X. LLM-Pruner: On the Structural Pruning of Large Language Models. In *Neural Information Processing Systems (NeurIPS)*, 2023.

Maslej, N. et al. Artificial Intelligence Index Report 2025. Technical report, AI Index Steering Committee, Institute for Human-Centered AI, Stanford University, 2025.

Merity, S., Xiong, C., Bradbury, J., and Socher, R. Pointer Sentinel Mixture Models. In *International Conference on Learning Representations (ICLR)*, 2017.

Mugnaini, L. G. et al. Efficient LLMs with AMP: Attention Heads and MLP Pruning. In *International Joint Conference on Neural Networks (IJCNN)*, 2025.

Muralidharan, S. et al. Compact Language Models via Pruning and Knowledge Distillation. In *Neural Information Processing Systems (NeurIPS)*, 2024.

Sakaguchi, K., Le Bras, R., Bhagavatula, C., and Choi, Y. WinoGrande: An Adversarial Winograd Schema Challenge at Scale. *AAAI Conference on Artificial Intelligence (AAAI)*, 2020.

Schwartz, R. et al. Green AI. In *Association for Computing Machinery (ACM)*, 2020.

Sengupta, A., Chaudhary, S., and Chakraborty, T. You Only Prune Once: Designing Calibration-Free Model Compression With Policy Learning. In *International Conference on Learning Representations (ICLR)*, 2025.

Sheng, Y. et al. FlexGen: High-Throughput Generative Inference of Large Language Models with a Single GPU. In *International Conference on Machine Learning (ICML)*, 2023.

Sreenivas, S. T. et al. LLM Pruning and Distillation in Practice: The Minitron Approach. *arXiv*, 2024.

Touvron, H. et al. Llama 2: Open Foundation and Fine-Tuned Chat Models. *arXiv*, 2023a.

Touvron, H. et al. LLaMA: Open and Efficient Foundation Language Models. *arXiv*, 2023b.

van der Ouderaa, T. F. A., Nagel, M., van Baalen, M., and Blankevoort, T. The LLM Surgeon. In *International Conference on Learning Representations (ICLR)*, 2024.

Wang, F. et al. Layer as Puzzle Pieces: Compressing Large Language Models through Layer Concatenation. In *Neural Information Processing Systems (NeurIPS)*, 2025.

Yang, M., Lin, S., Li, C., and Chang, X. Let LLM Tell What to Prune and How Much to Prune. In *International Conference on Machine Learning (ICML)*, 2025.

Yang, Y., Cao, Z., and Zhao, H. LaCo: Large language model pruning via layer collapse. In *Empirical Methods in Natural Language Processing (EMNLP)*, 2024.

Yu, W. et al. MM-vet: Evaluating large multimodal models for integrated capabilities. In *International Conference on Machine Learning (ICML)*, 2024.

Zellers, R. et al. HellaSwag: Can a Machine Really Finish Your Sentence? In *Association for Computational Linguistics (ACL)*, 2019.

Zhang, K. et al. LMMs-eval: Reality check on the evaluation of large multimodal models. In *Findings of the Association for Computational Linguistics (NAACL)*, 2025.

Zhao, H. et al. LOVA3: Learning to visual question answering, asking and assessment. In *Neural Information Processing Systems (NeurIPS)*, 2024.